Electrosynthesis of Ni/Al Layered Double Hydroxide and reduced graphene oxide composites for the development of hybrid capacitors

Elisa Musella[1], Isacco Gualandi[1], Giacomo Ferrari[1], Davide Mastroianni[1], Erika Scavetta[1], Marco Giorgetti[1], Andrea Migliori[2], Meganne Christian[2], Vittorio Morandi[2], Reinhard Denecke,[3] Massimo Gazzano,[4] Domenica Tonelli[1*]

[1] Dipartimento di Chimica Industriale "Toso Montanari", Università di Bologna, Viale Risorgimento 4, 40136 Bologna, Italy

[2] Istituto per la Microelettronica e i Microsistemi (IMM), Consiglio Nazionale delle Ricerche (CNR), via Gobetti 101, 40129 Bologna, Italy

[3] Wilhelm-Ostwald-Institut für Physikalische und Theoretische Chemie, Universität Leipzig, Linnéstraße 2, D-04103 Leipzig, Germany

[4] Istituto per la Sintesi Organica e la Fotoreattività (ISOF), Consiglio Nazionale delle Ricerche (CNR), via Gobetti 101, 40129 Bologna (Italy)

[*] Corresponding author

Abstract

An electrochemical synthesis which has been optimized to produce layered double hydroxides (LDHs) intercalated with carbon nanomaterials is proposed for the first time.it is based on a one-step procedure which contemporaneously allows for the Ni/Al-LDH synthesis, the reduction of graphene oxide (GO) and its intercalation inside the structure. The LDH/ERGO composites were thoroughly characterized by a comprehensive multi-techniques approach in order to verify their structure and morphology. The results confirmed that a LDH structure was observed only if the GO concentration was not higher than 2 mg/mL. All the characterizations led to propose a theorization of the synthetic and growth mechanisms of the composites. The best performing material was employed as cathode

for the development of a hybrid supercapacitor. The device had a discharge specific capacity of 880 F g^{-1}. The promising results obtained in this work embrace the necessity of development of low environmental impact systems; in fact, the proposed hybrid supercapacitor is binder-free, safe, composed of earth abundant elements and able to work in aqueous electrolyte.

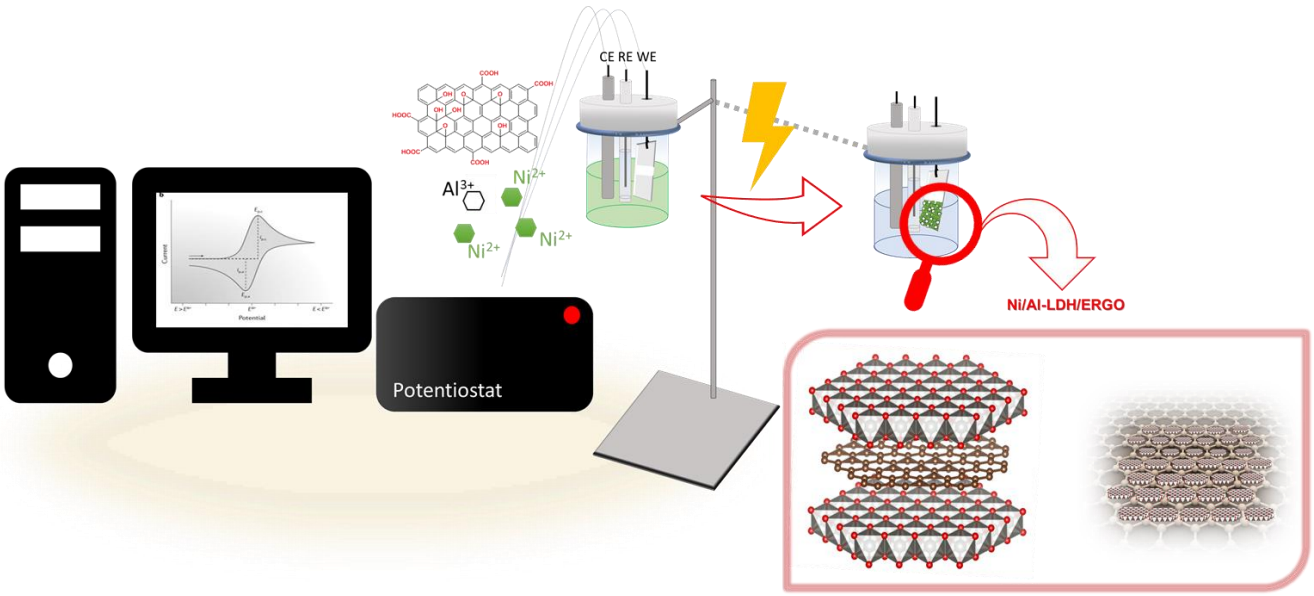

GRAPHICAL ABS

Introduction

The global energy demand doubles every 14.5 years and more than 60% of the electricity production is derived from coal and natural gas[1] with an associated huge emission of CO_2, which is considered the main contribution to greenhouse effect and global warming.

Because of such detrimental environmental effects, substituting fossil fuels with renewable energy sources has become a moral imperative. Since our reliance on renewable energy should grow in the next future, there are increasing research efforts to develop devices that store it for the times the energy cannot be harvested [2]. Currently, the commercial standard in energy storage is the pumped-hydro one, which exhibits some constrains because it is site-dependent and not widely available. Among possible alternatives, electrochemical storage plays a key

role and electrochemical supercapacitors are very promising devices that have been developed at demonstration level [3].

Nowadays, researchers are focusing their attention on finding new electrode materials in order to boost the performances of electrochemical supercapacitors. Environmental sustainability is also essential considering a possible large-scale production and diffusion. Since all harmful substances should be avoided, new eco-friendly devices are proposed in literature replacing the organic solvent with water or/and eliminating the binder that is exploited for the electrode preparation [4].

In this scenario, layered double hydroxides (LDHs) are promising materials, which can be described by the general formula $M(II)_{1-x}M(III)_x(OH)_2]^{x+}$ $(A_n^{x/n-})\cdot mH_2O$, where M(II) and M(III) are the metal cations that are bivalent and trivalent, respectively. The cations form 2D hydroxide layers wherein they exhibit an octahedral coordination which is the same of brucite [$Mg(OH)_2$]. Due to the M(III) presence, the hydroxide structure acquires a positive charge and anions A_n must be intercalated in the interlayers.[5] These compounds have been found to be extraordinary materials for great number of application, ranging from electrochemistry [6-8] to industrial catalysis [9,10] environmental decontamination,[11] drug delivery systems,[12] etc. In particular, if M(II) can undergo a redox process, LDHs become somewhat electrically conductive and they can be employed for the development of electrochemical technologies, for instance in the field of energy storage devices, [13-15] as electrode coatings for amperometric or potentiometric sensors [16-18] and as catalysts for water splitting reaction [19-21]. LDHs offer several intrinsic advantages, such as tuneable chemical composition and layered structure that should guarantee ion-exchangeability, efficient Faraday reaction, large surface area, relatively low cost and environmentally friendly features [5,7,14,22–30].

However, many LDH applications are still largely restricted due to the fact that they have low electrical conductivity [31–33]. Of course, this reduces the performance of electrochemical devices because the supercapacitor applications need high currents flowing during fast charge−discharge cycles. These weak points can be overcome by combining LDHs with carbon nanomaterials, such as graphene. Graphene is a single layer of carbon atoms arranged in a hexagonal lattice, which exhibits high accessible surface area, good electrical conductivity, chemical and thermal stability, and mechanical strength [34–37].

Several LDH/graphene composite materials were synthesized by bulk chemical synthesis[38] or assembled exploiting the opposite charge of carbon nanomaterials and brucite layers [13,39]. The resulting composites take advantage of the intrinsic conductivity of carbon nanomaterials and superior electrochemical features of LDHs to obtain a synergistic effect

that remarkably boosts their electrochemical performance [14]. For instance, it has been reported[40] that the addition of carbon nanomaterials into LDHs produces such an effect: the electron charge transport occurs through carbon skeleton, while the redox active hydroxides allow to have a high capacitance.

Moreover, the complementary structure of the two components hinders or slows LDH reorganization processes that take place during the operativity of the electrochemical devices based on LDHs, thus leading to an insufficient stability for real-life applications [33]. However, many problems are still present. In fact, powders are typically mixed with conductive additive and polymer binder to form pasted electrodes [41]. In the se cases, the actual capacity of the electrode tends to be lowered and the electrolyte accessibility to the active material is decreased due to the presence of the inactive components, which further devalue the electrochemical performance. A possible alternative is the direct growth of the active material on a conducting substrate, which usually enables good electrical contact and enhances the ion transport kinetics [41–45].

Electrosynthesis is a cheap, fast and environmentally friendly route to prepare LDHs directly on the electrode with well-adhered coatings.[9,10,17,24,46] Our group has worked on the LDHs electrosynthesis with a potentiostatic approach since 2004, [47] and applied the resulting chemically modified electrodes to sensing, energy storage and production, heterogeneous catalysis and oxygen evolution reaction. In spite of that, the potentiostatic route did not allow a perfect control of M(II)/M(III) ratio and did not assure an optimum reproducibility of the LDH films. Recently, [29,30,33] we have proposed a potentiodynamic method for the reproducible production of LDHs with complex and controlled structures. In particular, the research has been addressed to the synthesis of Co based LDHs and of a Ni based LDH electrodeposited on carbon nanomaterials modifying a GC support which has been successfully applied for glucose sensing.

In the present work, we propose an electrosynthetic protocol that produces nanostructured films by the simultaneous co-deposition of a Ni/Al-LDH and electrochemically reduced graphene oxide (ERGO) on a graphitic electrode. We utilized an electrode modified with a Ni based LDH in order to limit the use of Co in real devices, since it has become a critical constraint on the supply chain of the energy storage and conversion industry [48]. Al^{3+} can strengthen the M–O (M = Ni, Co) binding energy and offer a stable scaffold for the active sites to anchor the metal ions, which is beneficial for the redox reaction of LDH nanosheets. Furthermore, incorporating Al^{3+} into LDH layers can increase the crystallinity and hydrophilicity of the LDHs, resulting in enhanced electrolyte accessibility and charge

transportation [49]. The electrosynthesis procedure was optimized by varying the GO concentration in the bath and by thoroughly characterizing the obtained electrodeposited films. To the best of our knowledge, an electrochemical route able to intercalate a big structure in the LDH interlayers has never been reported before.

Moreover, we demonstrate the possibility to take advantage of the unique properties of the interpenetrated materials to be applied in an eco-friendly energy storage device that successfully works in aqueous electrolyte without the presence of a binder.

Materials and Methods

Chemicals

Nickel (II) nitrate hexahydrate, aluminium nitrate nonahydrate (>96% pure), graphene oxide (4 mg/mL in water dispersion), polyvinyl alcohol (>99% pure), polyvinylidene fluoride (PVDF) and activated carbon (AC) were supplied by Sigma-Aldrich. Sodium hydroxide (98% pure) and potassium hydroxide were purchased from Merck. Potassium chloride was produced by Fluka analytical. Acetylene black was purchased from Alfa Aesar. The supporting electrolytes for the electrochemical experiments were 0.1, 1, or 6 M KOH. The salt solutions were prepared with distilled water. Graphite GTJ (Graphite>99.8%) was used as the support and purchased from VED (https://www.ved.it).

Apparatus

Electrode potentials were measured with respect to an aqueous saturated calomel electrode (SCE) or with respect to a mercury-mercury oxide electrode (Hg/HgO). A Pt wire was used as the counter electrode. The curves were recorded by means of a CH Instruments Mod. 660C, controlled by a personal computer via CH Instruments software. Galvanostatic cycling with potential limitation in constant current mode was performed by using a battery cycler (Neware Battery Testing System).

Powder X-ray diffraction (PXRD) analysis was carried out by means of a PANalytical X'Pert PRO diffractometer equipped with a fast X'Celerator detector. Cu Kα radiation was used (λ=0.15418 nm, 40 mA, 40 kV). The 2-theta range was investigated from 5° to 60° with a step size of 0.066° and time/step of 250 s. The elemental analysis was performed using an Agilent 4210 Atomic Emission Spectrometer MP-AES, controlled by a computer via Agilent MP Expert software.

The morphology, structural and chemical compositions of the LDH films were investigated by Field Emission-Scanning Electron Microscopy (FE-SEM) using a LEO 1530 ZEISS

instrument equipped with Schottky emitter, operated at an acceleration voltage variable from 5 to 15 keV, and Everhart-Thornley and In-lens detectors for secondary electrons imaging. Energy Dispersive X-ray Spectroscopy (EDS) measurements were performed with an Oxford INCA system equipped with a 30 mm^2 Silicon Drift Detector. The Transmission Electron Microscopy (TEM) analyses were performed with a FEI TECNAI F20 microscope endowed with Schottky emitter and operated at 200 keV. The instrument is also equipped with EDS and Scanning Transmission Electron Microscopy (STEM) detectors. The TEM images were acquired in phase contrast mode while STEM images were recorded using a High Angle Annular Dark Field (HAADF) detector and show an intensity I that is proportional to $Z^{1.7}t$, where Z is the mean atomic number and t is the thickness of the specimen (the so-called Z-contrast). The specimens for TEM observations were prepared by scratching the films deposited on the platinum support with a blade. The powder thus obtained was then dispersed onto a holey carbon film supported by copper grid.

Infrared spectra were recorded on a Perkin Elmer Spectrum 2000 FT-IR spectrophotometer. In order to study the surface composition of the two selected redox active materials (LDH/ERGO0.05 or LDH) for the supercapacitor development, X-ray Photoelectron Spectroscopy (XPS) was used. The spectra were recorded with a VG ESCALAB 220 iXL spectrometer. The X-ray source was non-monochromatized Al Kα. During the experiment the base pressure was 1×10^{-8} mbar. Detail spectra of relevant core levels were scanned four times at a pass energy of 10 eV with a step width of 0.1 eV and a dwell time of 300 ms. The detail spectra were corrected by subtraction of excitation satellites before peak fitting due to the non-monochromatized Al anode. Data analysis was performed by UNIFIT 2020 (https://www.unifit-software.de/). The background of the detail spectra was fitted using a combination of polynomial and Shirley background. Peak shapes were simulated combining Lorentzian and Gaussian functions by convolution (Voigt profile). The binding energy scale was calibrated to the C 1s signal of adventitious hydrocarbons at 285.0 eV.

Preparation of chemically modified electrodes

Cleaning the electrode is a critical step to achieve a well adherent coating. For Pt electrodes, the surface was first polished to a mirror-like surface by a mechanical cleaning, using sand-paper, and then the electrode was submitted to an electrochemical treatment: 250 cycles between -0.25 V and +1.30 V were performed in 0.1 M H_2SO_4 at a scan rate of 1 V s^{-1}. For the graphitic electrode (Grafoil), the surface was rinsed in ethanol for 10 min and then dried to constant weight.

The LDH films were deposited on the electrode surface by cathodic reduction of a freshly prepared 0.03 M solution containing Ni and Al (from nitrate salts) at a molar ratio of 3:1 with a scan rate of 25 mV s^{-1} between 0 and -1.3 V vs SCE.

The co-deposition of LDH and ERGO was carried out in three different ways (Figure 1a), using the same parameters adopted for the synthesis of the pure LDH: the metal salt concentration was always kept constant while decreasing amounts of GO were employed. In particular, LDH/ERGO1, LDH/ERGO0.2, LDH/ERGO0.05 mean that the GO into the starting solution was 1, 0.2, 0.05 mg/mL.

After performing the modification, the electrode was immediately rinsed with water.

Preparation of the hybrid supercapacitor

The asymmetric hybrid supercapacitor (SC)is composed by two different electrodes:

- LDH/ERGO0.05 or LDH on Grafoil
- Activated carbon (AC) based electrode

For the fabrication of the latter, the selected formulation is 0.7g of AC, 0.2 g of Acetylene Black (AB) and 0.1 g of PVDF. The obtained slurry is dispersed on a 3x3 (device in solution) or 2x2 (assembled SC) cm^2 area of Grafoil.

When the SC performances are evaluated in solution, the two electrodes are immersed in 6 M KOH using two terminal device setting. The mass loading of Ni/Al-LDH was 0.3 mg whereas for the LDH/ERGO0.05 was 0.7 mg.

When the SC has been assembled, a solid polyelectrolyte has been used. It has been prepared with the following procedure:

1. weight 1 g of PVA, 0.001 mol of KOH, and 0.001 mol of KCl
2. transfer the reagents in a 10 mL flask and take to volume with distilled water
3. stir for 10 minutes at 100-150°C
4. transfer the mixture to a Petri dish and let it dry overnight.

Prepare a square polydimethylsiloxane mask of 3x3cm^2 area. Remove the central part, leaving an internal square of 2x2 cm^2 area. Fix the mask on a 3x6cm^2 area Grafoil sheet and fill the internal part with the AC based slurry. Let the slurry dry. Fill the hollow with the solid polyelectrolyte. Then fix the Grafoil sheet modified with the electrodeposited LDH or LDH/ERGO0.05 on the upper part (see figure 9a).

Results and Discussion

Electrochemical deposition

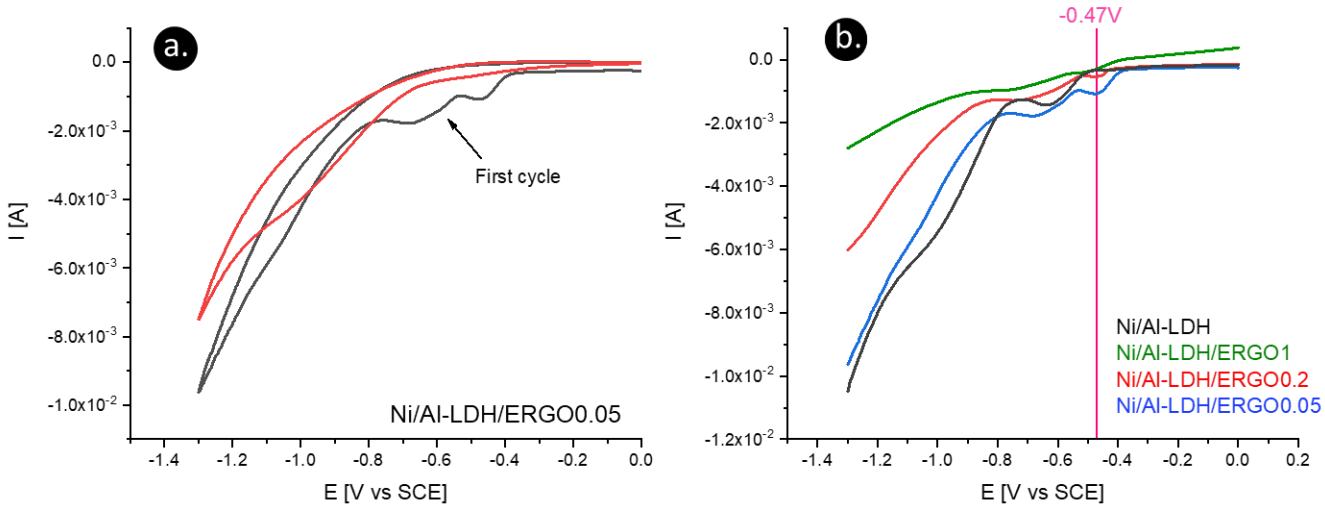

Figure 1: a) CV curves recorded during the electro-deposition of Ni/Al-LDH on Pt, in the presence of a GO concentration of 0.05 mg/mL. b) Comparison of the first sweeps recorded during the electrodeposition of Ni/Al-LDH, Ni/Al-LDH/ERGO0.05, Ni/Al-LDH/ERGO0.2, and Ni/Al-LDH/ERGO1

The LDH/ERGO electrodeposition is performed by applying a variable potential ranging from 0.0 V to a cathodic value (-1.3 V vs SCE) to the electrodes while they are immersed in a solution containing the nitrate salts of the metals Ni^{2+} and $Al^{3+}$and GO. The negative polarization has hereby a dual purpose:

i) to induce the reduction of nitrates and water according to reactions 1−7 [50];

1. $H^+ + e^- \rightarrow H_{ads}$
2. $2H^+ + 2\ e^- \rightarrow H_2$
3. $NO_3^- + 2H^+ + 2e^- \rightarrow NO_2^- + H_2O$
4. $NO_3^- + 10H^+ + 8e^- \rightarrow NH_4^+ + 3H_2O$
5. $2H_2O + 2e^- \rightarrow H_2 + 2OH^-$
6. $NO_3^- + H_2O + 2e^- \rightarrow NO_2^- + 2\ OH^-$
7. $NO_3^- + H_2O + 8e^- \rightarrow NH_4^+ + 10\ OH^-$

ii) to reduce graphene oxide present in the solution in order to restore its conductivity properties (reaction 8).

8. GO → ERGO

The reactions 1-7 cause the H^+ depletion and OH^- production: this means that the pH shifts from an acidic to a basic value, which leads to the LDH precipitation on the electrode surface. This involves both the nucleation and growth of crystals, as typical of all the solubility equilibria. Therefore, the rate of the process is controlled by the oversaturation degree of the solution and by the presence of defects on the electrode surface that can act as nucleation centers [51]. Furthermore, the Ni/Al-LDH precipitation can follow two different pathways depending on the rate of pH increase. If the pH increases slowly, $Al(OH)_3$ precipitation takes place first, and when all the Al^{3+} has been completely consumed, the bivalent cations can be inserted into the amorphous structure of $Al(OH)_3$ to form the layered structure [24]. However, direct precipitation can occur when a quick pH variation occurs [46].

The voltammograms recorded during the deposition of Ni/Al-LDH/ERGO0.05 are displayed in figure 1a. It is important to highlight that, in the cathodic sweep of the first cycle, it is possible to observe three peaks, two of them already present in the deposition trace recorded for the LDH alone (at about -0.65 and -1 V, figure 1b). The third peak is located at -0.47 V vs SCE and we suggest that it can be ascribed to the reduction of GO to ERGO. Moreover, in the first sweeps of all the CVs relevant to the electrosynthesis of the composites the current decrease is proportional to the quantity of GO in solution (this is also true for the second cycle, see SI 1). In particular, it is reasonable to guess that the reduction of GO competes with the one of nitrates: considering a concentration of 1 mg/mL, the reduction peak at -0.47V is barely detectable. Therefore, the argument behind the hypothesis is that the reduction of the GO poorly takes place and even that it hinders the nitrate reduction necessary for the pH increase and, therefore, for the LDH electrodeposition. This hypothesis is confirmed by PXRD (see below). Moreover, the molar ratio Ni/Al has been evaluated by means of MP-AES and resulted: 3.03 for the pure LDH, 2.93 for Ni/Al-LDH/ERGO0.05, 1.63 Ni/Al-LDH/ERGO0.2 and 0.95 for Ni/Al-LDH/ERGO1.These data suggest that only in case of the highest GO concentration the Ni/Al ratio is not compatible with a LDH structure. It is, therefore, clear that for the electrosynthesis of a LDH/ERGO composite, it is fundamental to choose the proper GO concentration in solution. In fact, the reduction of GO should interfere as little as possible with the reduction of nitrates, thus guaranteeing the adequate pH for LDHs precipitation. If it is not the case then an amorphous phase containing $Al(OH)_3$, where only a partial insertion of Ni^{2+} has occurred, precipitates on the electrode instead of a LDH.

Structural characterization

The thin films obtained by potentiodynamic synthesis were characterized by PXRD to confirm the formation of a LDH structure. The diffractograms of all the composite materials are plotted

in figure 2a. All of them, except for LDH/ERGO1, display the two typical reflections, indexed as 006 and 003, and reveal good phase formation.

Peak positions are all different one each other. As already reported in literature,[52] the intercalation of ERGO into the LDH is confirmed by a decreased interlayer distance. In particular, d values are calculated to be 0.88 nm for Ni/Al-LDH, whilst 0.83 nm for LDH/ERGO0.02 and 0.81 nm for LDH/ERGO0.05. The same trend has been observed, for a Ni/Al-LDH graphene composite synthesized by a chemical synthesis based on layer by layer stacking of the two materials [52].

As stated above, our results might suggest that the lower GO concentration is in the deposition solution the higher is its degree of reduction and also its interlayer intercalation, due to the strong electrostatic interaction between ERGO and LDH sheets, leading to a thinner spacing between the brucite-like layers.

Figure 2b shows that all samples present almost the same absorption peaks in the FT-IR spectra. The relatively strong and broad peak between 3700 and 3200 cm^{-1} is related to the O–H stretching vibration of Ni–O–H, and the broad absorption peak at 1630 cm^{-1} is associated to the O–H stretching and bending vibrations of the interlamellar water molecules due to the formation of hydrogen bonds. The weak bands below 800 cm^{-1} are assigned to lattice vibrations of metal-oxygen (M–O) in the brucite-like layers [53,54]. The band at 1100 cm^{-1} can be ascribed to the epoxy bonding C-O-C, and, therefore, is the most suitable to point out the presence of GO at different extent of reduction [52]. As a matter of fact, it is possible to notice that the intensity of this band increases with GO concentration in the starting solution. Independently from the real structure of the composite Ni/Al-LDH/ERGO this observation leads to furtherly confirm that when the GO concentration is at the highest value (1mg/mL) the electrochemical reduction of the oxygen containing functionalities is not so efficient as when the concentration is lower (0.05 and 0.2 mg/mL), as already discussed in the previous section. The obvious conclusion is that the concentration of 1 mg/mL is too high for the preparation of a composite LDH/ERGO, since it both hinders the LDH precipitation and the GO reduction. A possible explanation to this behaviour can be seen in the low conductivity of graphene oxide itself. In fact, when the GO concentration is the highest, the conductivity of the overall system could be affected, thus leading to the need of a higher overpotential for the reduction occurrence. Moreover, GO might also be adsorbed on the electrode surface causing a decrease in its active area.

Finally, the absorption bands located at about 1380 cm^{-1} correspond to the stretching vibrations of N-O (nitrate ions) and are present in all the materials, except for LDH/ERGO1,

although with different relative intensities.[55] In any case, the presence of interlayer nitrate anions is not in conflict with PXRD data: the reflections are so broad that a contribution of the nitrate could not be neglected.

Indeed, also GO has absorption bands [56] at 1387.5 and 1418.8 cm^{-1} and, actually, they are detectable in the spectrum of LDH/ERGO1, so furtherly confirming that, in these synthesis conditions, the GO reduction practically does not occur.

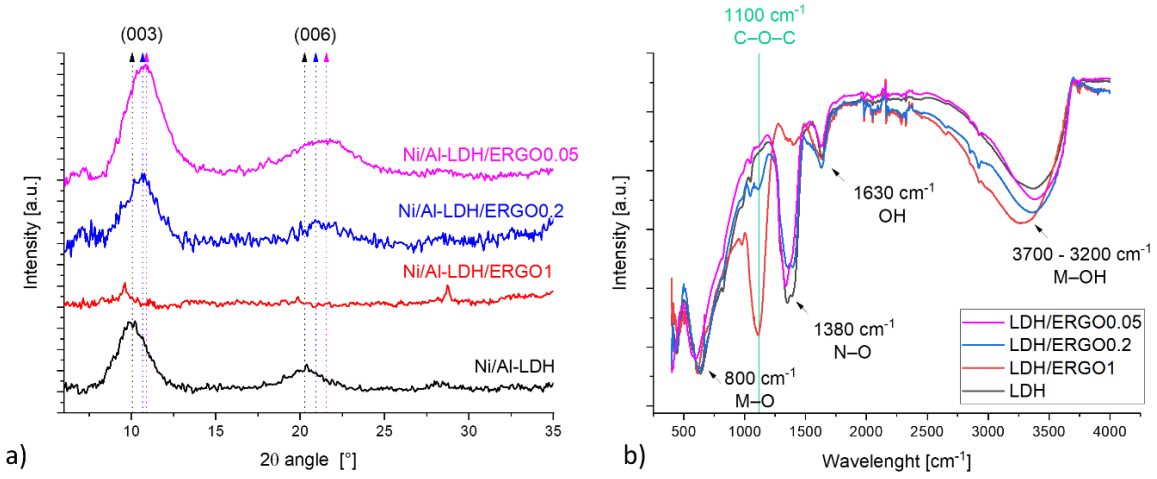

Figure 2: a) PXRD and b) FT-IR spectra of all the set of samples

Morphological Characterization

The morphology of the LDH films was investigated by FE-SEM. Figures 3a-d show the images of electrodeposited thin films coming from the three electrolytic solutions with GO different concentration. Figure 3a shows that the pure Ni/Al-LDH displays a homogeneous and compact layer with a nanostructured surface due to the very small LDH crystallites (around 40 nm). The thickness of the layer can also be estimated to be around 200 nm. Nanostructured surfaces are shown also in Figures SI2 – SI5 for Ni/Al-LDH, Ni/Al-LDH/ ERGO1, Ni/Al-LDH/ ERGO0.2, and Ni/Al-LDH/ ERGO0.05 respectively.

LDH/ERGO1 exhibits a structure typical of a graphitic like nanomaterial on which an inorganic compound has been deposited in a non-homogeneous way. In fact, it is possible only to observe some aggregates of the aluminium rich amorphous material, whose existence has been already widely discussed. The presence of GO, due to the poor reduction, is predominant here. (Figure 3b) At higher magnifications (SI3), it can be also observed some inorganic material under a layer of GO. From the cross-sectional image of LDH/ERGO0.2 composite (Figure 3c), it is possible to point out a complex structure. In fact, starting from the electrode surface (bottom) it visible a uniform LDH layer, covered with ERGO flakes on

which a thick deposit of LDH has grown, and finally another ERGO sheet on the top. Looking at the thick deposit it is possible to notice the presence of ERGO flakes strongly interconnected with the LDH particles.

ERGO is recognizable by its wrinkled surface, which is due to the rearrangements occurring after the removal of the hydroxyl and epoxy functionalities from the GO and the consequent recovery of the conjugated systems during the reducing process. This feature is even more evident in the case of LDH/ERGO0.05 (Figure 3d) where the two materials seem to exhibit the highest interpenetration and reduction degree. As far as TEM analysis is concerned (Figure 3e-f), the pure LDH displays again a granular structure in the thin border (Figure 3e), typical of this material, and a uniform distribution. In addition, even if the ordered structure is not clearly shown in the image, the Selected Area Electron Diffraction (SAED) pattern (SI6) clearly shows that two diffraction rings are detected with d=0.25 nm and d=0.15 nm, which furtherly confirms the LDH phase.[57] Figure 3f displays Ni/Al-LDH/ERGO0.05 sample: the presence of both ERGO and Ni/Al-LDH is again evident. SAED diffraction pattern shows four diffraction rings: d=0.25 nm, d=0.21 nm, d=0.15 nm and d=0.12nm. The rings with d = 0.21 and 0.12 nm (also in the Fast Fourier Transform, FFT, in the bottom left inset) can be indexed as the (1,-1,0) reflection of ERGO (or graphite – like compounds) (SI7).[58]

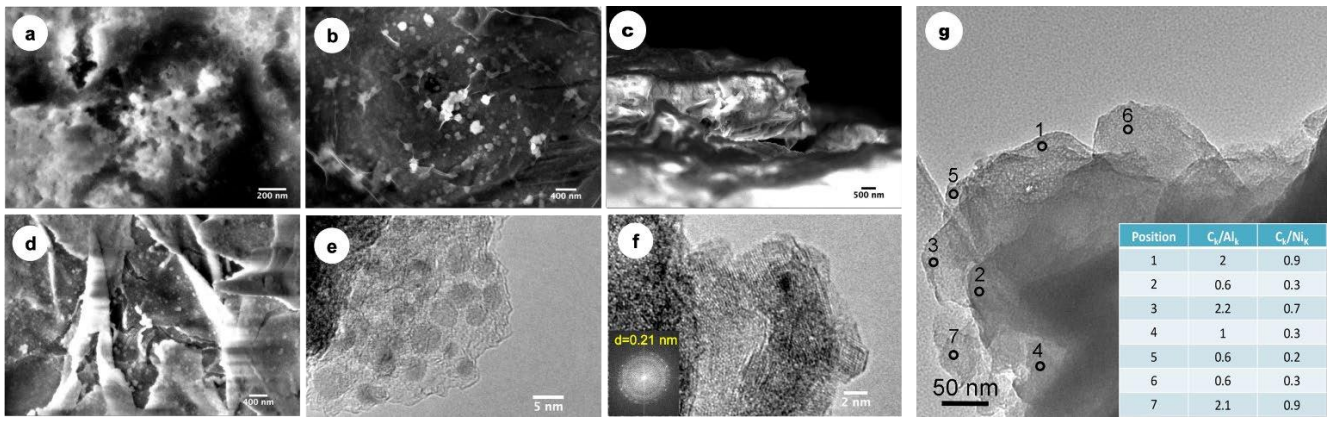

Figure 3: SEM images of a) Ni/Al-LDH b) Ni/Al-LDH/ ERGO1 c) cross-sectional view of Ni/Al-LDH/ ERGO0.2, and d) Ni/Al-LDH/ ERGO0.05. HREM-TEM images of e) Ni/Al-LDH, and f) Ni/Al-LDH/ ERGO0.05, inset: SAED pattern of ERGO g) TEM images of Ni/Al-LDH/ ERGO0.05; the open circles indicate the positions were the EDS spectra were collected. In the table the ratios between C_k/Al_k and C_k/Ni_K counts are shown.

Figure 3g reports phase contrast TEM image recorded on the border of a fragment which clearly displays a layered structure. Several EDS spectra were collected in the thinnest parts on the border. The seven positions are indicated with numbers from 1 to 7. The ratio between

the C_K and Al_K and Ni_K counts, as shown in the table, depends on the beam position, suggesting that the layers composition varies. This fact confirms that the compound is made up of layers having a different composition. Summarizing, these data, relevant to Ni/Al-LDH/ERGO0.2 and 0.05, support the hypothesis that a layer by layer growth of LDH and ERGO takes place, with also an interpenetration of ERGO sheets inside the inorganic material. Moreover, no nitrogen can be detected in this area, highlighting the nitrate absence.

XPS Characterization

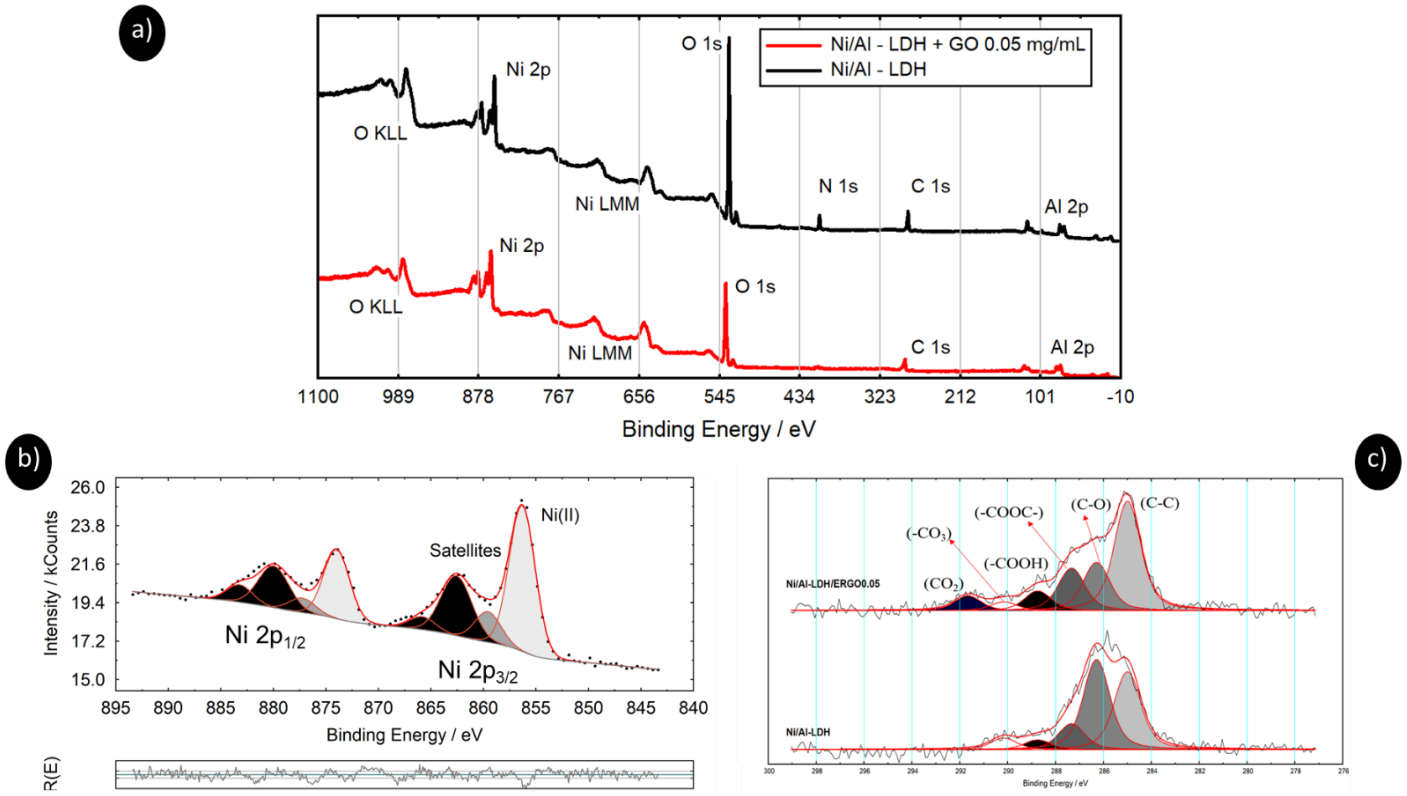

Figure 4: XPS data of a) normalized survey spectra of Ni/Al-LDH and Ni/Al-LDH/ERGO0.05 b) Ni 2p site of Ni/Al-LDH and c) comparison between C 1s of the pure LDH and LDH/ERGO0.05 composite (spectra have been normalized)

Figure 4 shows the XPS survey and high resolution Ni2p and C1s spectra of the pure LDH and the composite Ni/Al-LDH/ERGO0.05. A first difference between the materials can be seen already from the survey spectra: the signal of N1s is practically absent when GO is present in the electrolytic solution. This could be due to the fact that nitrate is not predominant in the first outer interlayer regions, having been replaced by ERGO. The Ni2p spectrum exhibits two main peaks at 856.4 and 874.0 eV, corresponding to $Ni2p_{3/2}$ and $Ni2p_{1/2}$, and the satellites. Of course, all Ni2p peaks are subject to spin-orbit coupling, which produces $2p_{3/2}$ and $2p_{1/2}$ peaks. In the case of $Ni(OH)_2$, the other

most important effect is multiplet splitting, which occurs because the unpaired core electron ($2p^5$) couples with the unpaired Ni^{2+} valence electrons ($3d^8$).[59] The spin-energy separation of 17.6 eV and the main peak located at 856.4 eV (Figure 4b) suggests the presence of Ni^{2+}, in good agreement with previously reported values for $Ni(OH)_2$.[60–63] The structure can be compared to the one of β-$Ni(OH)_2$,which is isostructural with brucite, $Mg(OH)_2$ [59].

Al2p detailed spectrum exhibits a peak at 74.5 eV (see Fig. SI8), which is in the reported binding energy range of $Al(OH)_3$.[64],[65] In particular, this position is related to gibbsite-type $Al(OH)_3$, which is structured in hexagonal closed packed sheets in which Al cation is octahedrally coordinated by 6 OH groups.[64] All these findings confirm the presence of Ni/Al-LDH. Ni2p and Al2p signals show no major difference for the material obtained in the presence of GO or the pure LDH.

The C1s spectra are expected to show a clear difference for the sample containing or not containing ERGO. As can be seen in Fig. 4c, this is indeed the case. However, as it is evident from the decomposition of the peaks into different contributions, both samples exhibit a complex structure. Most of the features correspond to carbon containing contaminations. The clearest evidence for the presence of ERGO is the strong contribution at about 285 eV (characteristic of C-C bonds in sp^2 configuration) but still C-O derived features above 286 eV (and even CO_2 or carbonate species around 292 eV) are present.[52, 66-69]

Discussion of the LDH/ERGO structure

On the basis of all the characterization data, the synthesized composites display a peculiar structure that should enhance the overall electrical conductivity.

The PXRD data exclude the LDH formation in the case of the composite named LDH/ERGO1. All the observations suggest that the reduction process of graphene oxide, even if occurring with low efficiency at the concentration of 1mg/mL (visible from the intense peak of epoxy group in IR spectrum), hinders the reduction of nitrates. The latter is responsible for the precipitation of LDH: as stated before, if the pH increases slowly at the electrode/solution interface, first amorphous $Al(OH)_3$ precipitation takes place and only when all the Al^{3+} has been completely consumed, it is possible for Ni^{2+} to enter the structure. Considering the resulting Ni/Al molar ratio, not compatible with a LDH structure (0.93), it is reasonable to conclude that this pathway has started but the nickel ion insertion in $Al(OH)_3$ has in large extent failed due to the too low pH value reached in the experimental conditions adopted for the preparation of this composite.

In the other two cases, PXRD suggests the formation of a poorly crystalline LDH/ERGO phase, where single ERGO foils are alternated with the brucite layers (from the decreased interlayer distance).

However, the reflections are so broad that a contribution of the nitrate presence in the interlayer region might not be neglected. In fact, as evident from IR data, NO_3^- is still present both in LDH/ERGO0.05 and in LDH/ERGO0.2. However, nitrogen has not been detected either by XPS on the outer surface (5-10 nm) of material on the electrode or by EDS analysis. A plausible explanation can be suggested thinking about the electro-synthetic mechanism: it is a complex multistep process. When the fast electrosynthesis is blocked, and thus the production of hydroxy ions, the still growing film can be somewhere contaminated by intermediate products which cannot be converted into LDHs. Since their structure is amorphous, they might have entrapped some NO_3^- inside them.

As stated before, the efficiency of the reduction processes increases with decreasing GO concentration in solution, as confirmed both from deposition CVs and from the signal of epoxy-groups in IR spectra.

Even though an intensive characterization effort has been performed it is hard to fully explain the two LDH/ERGO composite structures, due to the several competing processes involved in their synthesis. Combining PXRD data, CVs and SEM images, it is possible to highlight two different growth mechanisms. On one hand, ERGO is intercalated in the interlayer of the LDHs, on the other hand, ERGO acts as nucleation centre for the growth of the LDH. The lower is the concentration of GO in solution, the higher is the degree of reduction obtained and also its intercalation in the interlayers. It is possible to guess that the predominant mechanism for LDH/ERGO0.05 synthesis is the intercalation, whilst for LDH/ERGO0.2 is the crystallite growth of the LDH on the ERGO flakes.

Electrochemical Characterizations

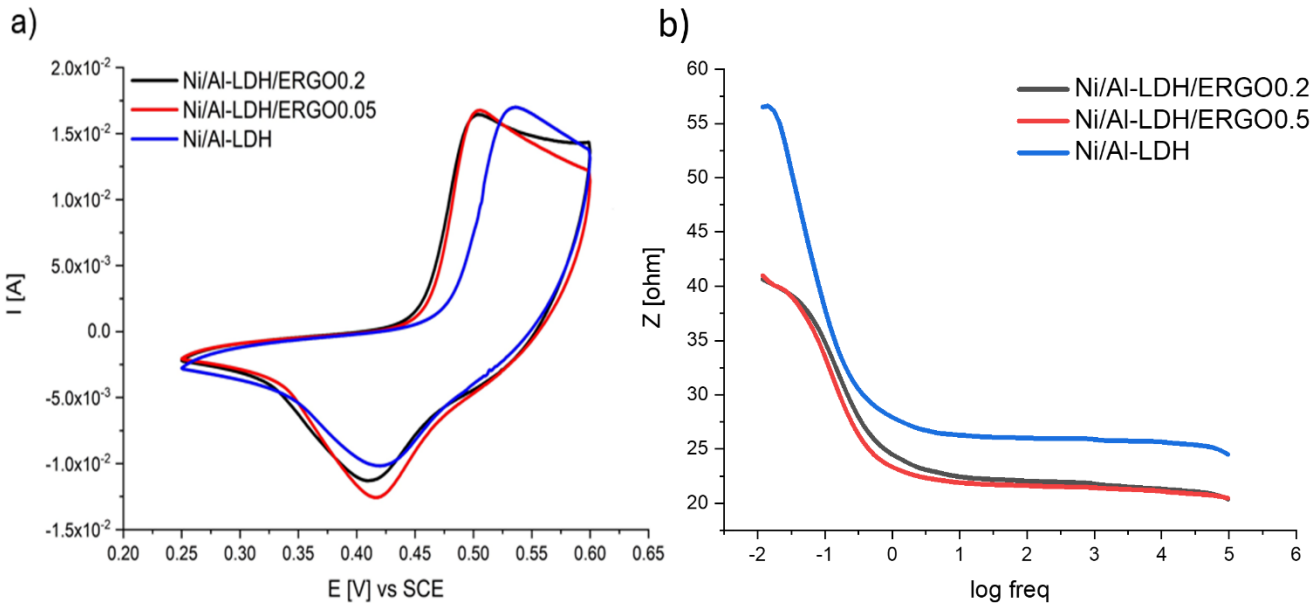

Figure 6: a) CVs of pure LDH and the composites Ni/Al-LDH/ERGO0.05 and Ni/Al-LDH/ERGO0.2 recorded at 10 mV/s; b)Bode plot for the same materials recorded when the applied potential corresponds to the maximum of the peak.

The CV characterization curves of the pure LDH and the two composites LDH/ERGO are reported in figure 6a. Cyclic-voltammograms display a typical reversible signal in the potential range between 0.25 and 0.6V, relative to the redox couple Ni(II)/Ni(III) involved in the electrochemical process described in Equation 9 [17]:

$$\mathrm{Ni(II)Al-LDH + OH- \rightleftarrows Ni(III)Al(OH)-LDH + e-} \qquad (9)$$

The presence of ERGO decreases the overpotential needed for the occurrence of the half reaction of Ni(II) oxidation with respect to the LDH alone. In fact, the anodic peak potential (E_{pa}) shifts from 0.52V toward 0.48 V. However, the amount of nanomaterial present in the electrolytic solution used for the synthesis does not seem to affect the performances: just a really low amount of ERGO (0.05 mg/mL) causes an enhancement of the reversibility of the system, suggesting that a further study on the comparison between Ni/Al-LDH and Ni/Al-LDH/ERGO0.05 can be very interesting. The crucial role of nanomaterials is demonstrated by the difference between the anodic and cathodic peak potentials (ΔE_p) of Ni/Al-LDH/ERGO0.05 that is lower than the value recorded for Ni/Al-LDH, at all investigated scan rates(1, 5, 10, 25, 50 and 100 mV/s). Since the charge transfer kinetics plays a key role in the fast power release, a study was performed to estimate the effect of intercalated ERGO

(see SI1). The ratio between the apparent charge transfer constant (k_s) of Ni/Al-LDH/ERGO0.05 and Ni/Al-LDH results equal to 25, so highlighting the superior features of the hybrid material in energy storage applications.

Electrochemical Impedance Spectroscopy (EIS) tests were performed at the anodic peak position, where the response is ruled by Ni redox process (equation 9), to gain more insights about the ERGO effects on the charge transfer processes taking place at Grafoil modified electrodes. Figure 6b, shows |Z| vs log (frequency) for Ni/Al-LDHs (blue curve), Ni/Al-LDH/ERGO0.2 (black curve) and Ni/Al-LDH/ERGO0.05 (red curve) to explicitly show the dependence of the overall impedance on the frequency. Looking at the graph, it is evident that ERGO presence lowers the impedance, especially in the low frequency region, that is connected to the kinetics of interfacial charge transfer reactions. This result confirms that ERGO, independently from its concentration (the curves obtained for 0.05 and 0.2 mg/mL ERGO concentration are practically superimposable) helps to improve the kinetics of Ni centers redox reaction.

Charge storage capability and hybrid electrochemical capacitor development

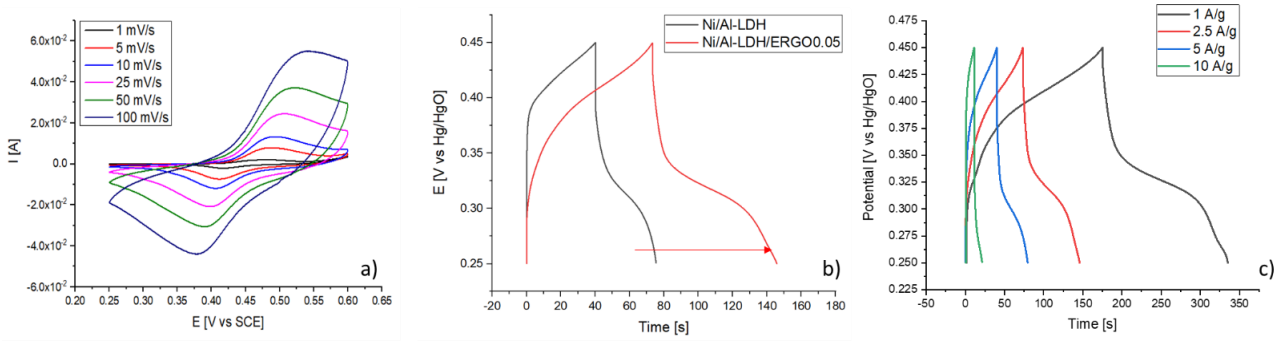

Figure 7: a) CVs at different scan rates of Ni/Al-LDH/ERGO0.05 in 0.1 M KOH; b) comparison of GC-D curves of Ni/Al-LDH/ERGO0.05 and Ni/Al-LDH at 2.5 A g^{-1}c) GC-D curves recorded at different current densities for Ni/Al-LDH/ERGO0.05.

In addition to the Faradaic process described in the above section, we have explored the charge storage characteristics of the deposited films to verify their possible application in hybrid electrochemical capacitors, as already reported for other layered double hydroxide materials.[25,66,70,71]

The electrochemical properties of the electrodes were initially investigated in a three-electrode cell using 0.1 M KOH as the supporting electrolyte. Figure 7a shows CVs at different scan rates.

The power-law relationship with the scan rate is:

$$i = av^b \qquad (10)$$

where i is the average current of anodic and cathodic peaks, ν the scan rate, and a and b are adjustable parameters. b values are calculated to be 0.76 for Ni/Al-LDH, and 0.78 for Ni/Al-LDH/ERGO0.05. These values indicate that the electrochemical behaviour of the two materials is controlled by both capacitive (b=1) and diffusive (b=0.5) processes. Figure 7b shows the galvanostatic charge/discharge (GC-D) curves that are recorded in 6 M KOH at the electrodes exploiting the pure LDH and LDH/ERGO0.05 in the potential range of 0–0.50 V. The potential windows were chosen in order to highlight the typical behaviour of the Faradaic process involving the LDH redox centres.

However, as can be seen better from Figure SI9, which displays a wider potential window, LDHs can also exhibit a linear variation of the potential (and thus the charge) with time, in addition to the Faradaic process (voltage plateau behaviour). Moreover, the charge increases in the presence of ERGO, underlying the merit of the present synthetic approach. At the current density of 2.5 A g^{-1}, the specific capacitances (Cs) of Ni/Al-LDH and Ni/Al-LDH/ERGO0.05 are 550 F g^{-1} and 650 F g^{-1}, respectively. The GC-D curves at different energy densities are reported in Figure 7c for the composite Ni/Al-LDH/ERGO0.05. C_s values result to be 745, 649, 600, 585 F g^{-1} at current densities of 1, 2.5, 5, and 10 A g^{-1}. It can be noticed that they decrease gradually with increasing current density, due to diffusion which limits the movement of the electrolyte ions [72]. Nevertheless, the materials retain a good rate in their performances. In all studied cases, when the current is reversed from charge to discharge, an ohmic drop occurs due to the internal resistance. The IR drop is slightly decreased in the case of Ni/Al-LDH/ERGO0.05 in respect with pure Ni/Al-LDH (see figure 7b).

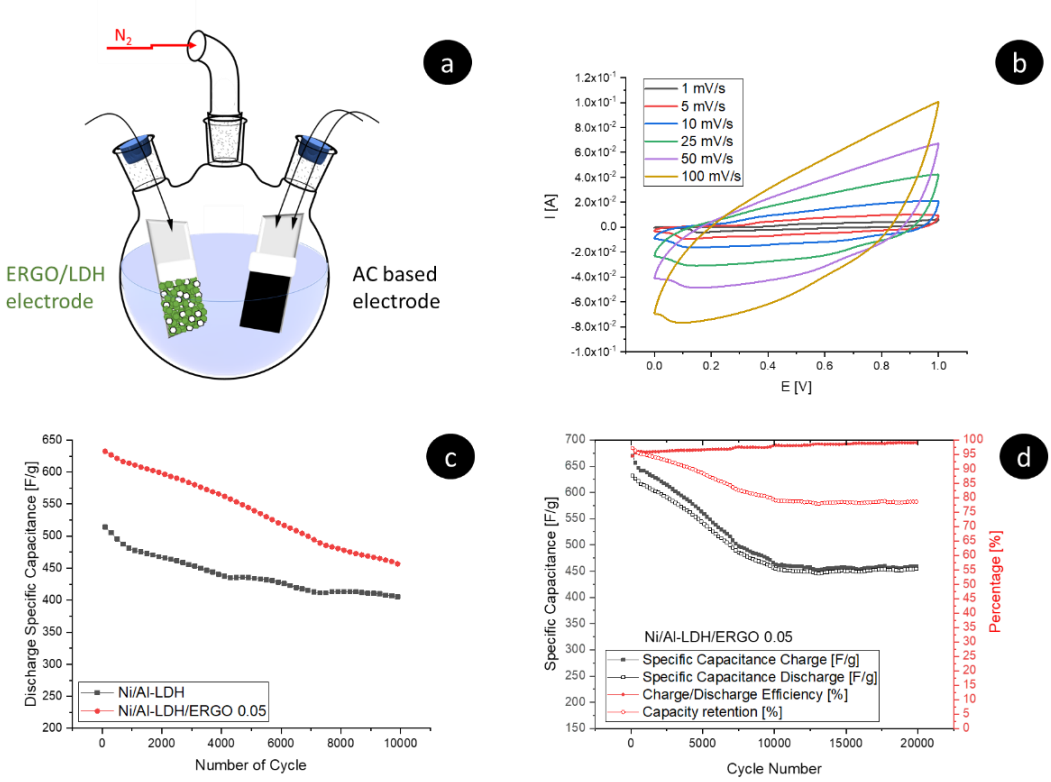

Figure 8: a) sketch of the set-up of the hybrid SC in solution; b) CVs at different scan rates of the asymmetric capacitor based of AC and Ni/Al-LDH/ERGO0.05 in 6 M KOH; c)comparison of the specific capacitance of Ni/Al-LDH and Ni/Al-LDH/ERGO0.05 during the continuous charge discharge cycling test at 2.5 A g^{-1}; d) capacitance retention of Ni/Al-LDH/ERGO0.05 at 2.5 Ag^{-1} for 20,000 cycles in solution.

The electrodeposited material was coupled to an AC electrode and tested in solution in a glass cell and in an assembled device as well. Figure 8a describes the configuration in solution, where the two electrodes, namely AC and Ni/Al-LDH/ERGO0.05, are immersed in 6 M KOH under nitrogen, whereas Figure 8b displays the CV responses recorded at different scan rate for this set up. All the CVs display a nearly capacitive behaviour in the potential range investigated, thus evidencing the charge storage capabilities of the hybrid supercapacitor when operating in solution. In figure 8c the specific discharge capacitance is plotted against the cycle number in a glass cell configuration by using the Ni/Al-LDH or Ni/Al-LDH/ERGO0.05 at one terminal side. Tests were made with a current density of 2.5 A g^{-1}. From this figure, a superior performance of Ni/Al-LDH/ERGO0.05 with respect to the pure LDH is evident. In both cases the specific capacitance decreases during the first 10,000 cycles but, as pointed out in figure 8d which shows also the charge capacity (black trace), it reaches a plateau after about 11,000 cycles at a value of 450 F g^{-1} for Ni/Al-LDH/ERGO0.05.

When using the composite material, the capacity retention over 20,000 cycle is around 80% and the charge/discharge efficiency is around 98% (red curves). Summarizing, even though the Ni/Al-LDH/ERGO0.05 electrode alone exhibits mainly a Faradaic behaviour, the experimental findings above described suggest that there is a room for the improvement and development of a hybrid supercapacitor when it is assembled with a capacitive electrode such as AC.

Table 1 compares the performances as supercapacitors in solution of different Ni/Al-based LDHs with and without the addition of carbon nanomaterials. Ni/Al-LDH alone has a specific capacitance in line with that of other chemically synthesized LDHs. Their C_s can be enhanced producing materials with peculiar morphology (such as hollow microspheres or petal-like structures) in order to favour the ion diffusion. The morphology effect is evident both for pure LDHs and composites.

The best capacitances are observed when nanostructured LDHs are produced in combination with 0D or 1D nanomaterials (nanoplates with quantum dots, nanosheets, etc…).

Anyway, our proposed composite shows better performances than LDHs combined with graphene or reduced graphene oxide as obtained in the form of bulk porous films (i.e., without controlled morphology).

The results of this work suggest that LDHs obtained with our method display capacitances that are definitively analogous to the chemically synthesized ones with uncontrolled morphology.

It is worth highlighting that our systems are particularly stable and long-lasting: they were still functioning after 20,000 cycles with respect to a maximum of 10,000 in other cases reported in the literature. Ni/Al-LDH/ERGO0.05 displayed the 80% of capacitance retention after 20,000 cycles which is the best stability obtained among all the compared materials. This high stability can be attributed to the strong adhesion to the supports, already demonstrated by us for LDHs electrosynthetic procedure [73].

Table 1: Comparison of the capacitive performances of the electrosynthesized Ni/Al-LDH and Ni/Al-LDH/ERGO0.05 with analogous chemically synthesized LDHs and C nanomaterials composites reported in the literature.

	Specific Capacitance F g^{-1} (at a specific current density A g^{-1})	**Capacity Retention (cycle numbers)**	**Electrolyte**	**Ref**
Pure LDHs				
NiAl-LDH petal-like	795 (2.5)	80% (1000)	1 M KOH	[74]
Hollow NiAl-LDH microspheres	735 (2)	116.5% (1000)	1 M KOH	[75]
NiAl-LDH	482 (10 mA cm^{-2})	94% (400)	6M KOH	[76]

NiAl-LDH	140 (0.4)	-	6M KOH	[77]
NiAl-LDH	550 (2.5)	69% (20000)	6M KOH	This Work
LDHs combined with carbon nanomaterials				
Quantum dots - NiAl-LDH nanoplates	1794 (2)	93% (1500)	6 M KOH	[78]
NiAl-LDHs - graphene nanosheets	1255.8 (1)	106% (1500)	6 M KOH	[79]
NiAl LDHs/g-C3N4	714 (0.5)	82% (10 000)	6M KOH	[80]
Flower-like NiAl LDH-NF/Graphene	214.7 (1)	80% (5000)	6M KOH	[81]
Ni/Al-LDH and rGO	39.55 (1.04)	67.4% (10000)	6 M KOH	[82]
Ni/Al-LDH/ERGO0.05	650 (2.5)	80% (20000)	6 M KOH	This work

Finally, figure 9a displays the first attempted device based on Ni/Al-LDH/ERGO0.05 electrode and AC which can be described as an all solid-state hybrid supercapacitor. In figure 9b, the first 1,500 cycles of the assembled hybrid supercapacitor are displayed as proof of concept. The capacitor has a starting discharge C_s of 880 F g^{-1} which decreases and stabilizes at 820 F g^{-1} after 300 cycles. The capacity retention is 88% and the charge/discharge efficiency is around 95%. Therefore, it is shown that the Ni/Al-LDH/ERGO0.05 material can be used as an electrode material for hybrid supercapacitors with interesting performance.

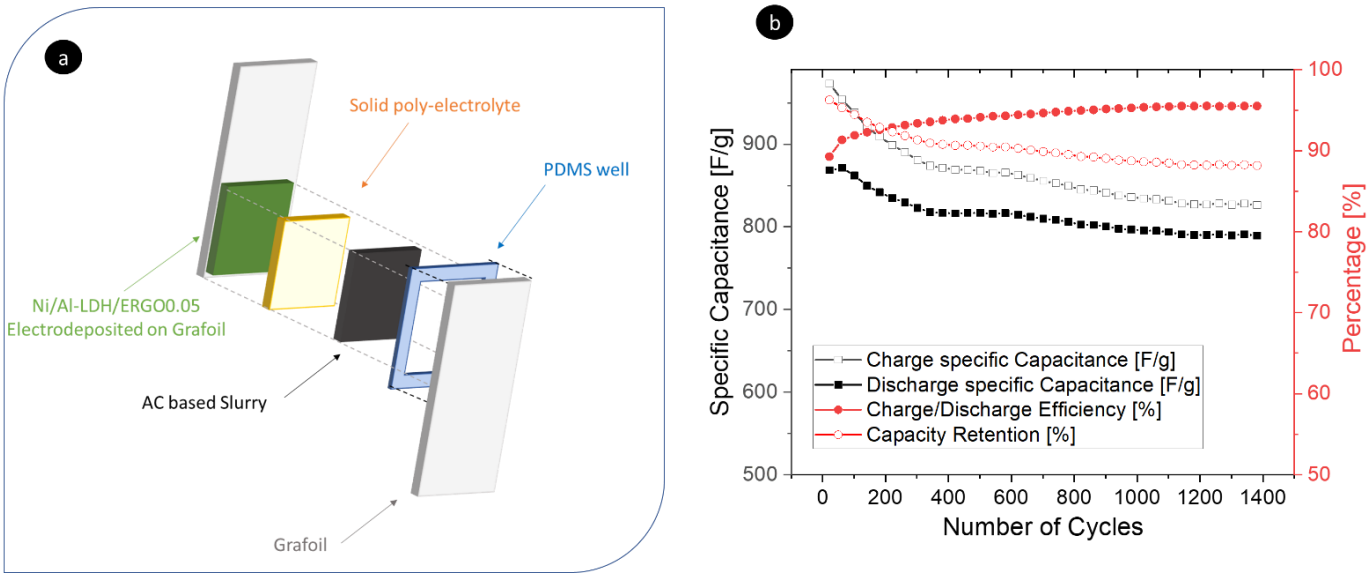

Figure 9: a) schematic representation of the hybrid SC; b) capacitance retention of the assembled SC at 2.5 A g^{-1} for 1,400 cycles

Conclusion

LDHs are promising materials in energy storage thanks to ion-exchange ability, high active area, and chemical tuneability. Electrosynthesis allows for the direct LDH growth on conductive surfaces with a green one-step procedure that does not require harsh conditions and additional compounds, such as a binder. Nevertheless, it has been exploited only for the preparation of LDHs with small intercalated anions, and thus the ability to tune chemical composition is significantly limited. We have explored a new protocol for the electrosynthesis of Ni/Al-LDHs intercalated with electrochemically reduced graphene oxide. The procedure has been optimized by varying the electrolytic solution composition. The ERGO intercalation has been proven by a comprehensive multi-technique approach demonstrating for the first time the possibility of electrosynthesis of LDH intercalated with big anions. The cyclic voltammetric characterization of Ni/Al-LDH/ERGO0.05 shows a higher reversibility than Ni/Al-LDH/NO_3 due to a boosted charge transfer that is enhanced by the ERGO presence. A hybrid capacitor has been fabricated both in solution and in solid-state. The robust structure of the composite ensures a long cycle life, making Ni/Al-LDH/ERGO0.05 very attractive as electrode material for hybrid supercapacitors. This work has highlighted a strategy to enlarge the spectrum of LDHs that can be prepared by electrodeposition and applied in many fields, such as energy storage, catalysis, sensors, and batteries.

Acknowledgement

The authors are grateful to the University of Bologna, Italy, for providing financial support. The authors are also grateful to Thomas Ruf for the help given in XPS measurement. The European Union's Horizon 2020 Research and Innovation Program (Grant Agreement no. 696656 Graphene Flagship) is acknowledged for funding. This research was also funded by the Italian Ministry of Research (MIUR) within PRIN-2015Project no. NEWLI2015CL3APH.

Bibliography

[1] M.D. Leonard, E.E. Michaelides, D.N. Michaelides, Energy storage needs for the substitution of fossil fuel power plants with renewables, Renew. Energy. 145 (2020) 951–962. https://doi.org/10.1016/j.renene.2019.06.066.

[2] I. Roger, M.A. Shipman, M.D. Symes, Earth-abundant catalysts for electrochemical and photoelectrochemical water splitting, Nat. Rev. Chem. 1 (2017).

https://doi.org/10.1038/s41570-016-0003.

[3] T.M. Gür, Review of electrical energy storage technologies, materials and systems: Challenges and prospects for large-scale grid storage, Energy Environ. Sci. 11 (2018) 2696–2767. https://doi.org/10.1039/c8ee01419a.

[4] M. Conte, P.P. Prosini, S. Passerini, Overview of energy/hydrogen storage: State-of-the-art of the technologies and prospects for nanomaterials, Mater. Sci. Eng. B Solid-State Mater. Adv. Technol. 108 (2004) 2–8. https://doi.org/10.1016/j.mseb.2003.10.107.

[5] P. Nalawade, B. Aware, V.J. Kadam, R.S. Hirlekar, Layered double hydroxides : A review, 68 (2009) 267–272.

[6] Y. Zhang, S. Wei, Mg-Co-Al-LDH nanoparticles with attractive electrochemical performance for supercapacitor, J. Nanoparticle Res. 21 (2019). https://doi.org/10.1007/s11051-018-4452-7.

[7] Zhengyang Cai,a Xiuming Bu,b Ping Wang,a,c,* Johnny C. Ho,b Junhe Yang,a,c Xianying Wang, Recent Advances on Layered Double Hydroxide Electrocatalysts for Oxygen Evolution Reaction, J. Mater. Chem. A. (2019). https://doi.org/10.1039/C8TA11273H.

[8] J. Martin, M. Jack, A. Hakimian, N. Vaillancourt, G. Villemure, Electrodeposition of Ni-Al layered double hydroxide thin films having an inversed opal structure: Application as electrochromic coatings, J. Electroanal. Chem. 780 (2016) 217–224. https://doi.org/10.1016/j.jelechem.2016.09.022.

[9] P. Benito, M. Monti, W. De Nolf, G. Nuyts, G. Janssen, G. Fornasari, E. Scavetta, F. Basile, K. Janssens, F. Ospitali, D. Tonelli, A. Vaccari, Improvement in the coating homogeneity in electrosynthesized Rh structured catalysts for the partial oxidation of methane, Catal. Today. 246 (2015) 154–164. https://doi.org/10.1016/j.cattod.2014.10.003.

[10] P. Benito, M. Monti, I. Bersani, F. Basile, G. Fornasari, E. Scavetta, D. Tonelli, A. Vaccari, Coating of FeCrAlloy foam with Rh catalysts: Optimization of electrosynthesis parameters and catalyst composition, Catal. Today. 197 (2012) 162–169. https://doi.org/10.1016/j.cattod.2012.07.034.

[11] F.L. Theiss, S.J. Couperthwaite, G.A. Ayoko, R.L. Frost, A review of the removal of anions and oxyanions of the halogen elements from aqueous solution by layered double hydroxides, J. Colloid Interface Sci. 417 (2014) 356–368. https://doi.org/10.1016/j.jcis.2013.11.040.

[12] F. Barahuie, M.Z. Hussein, S. Fakurazi, Z. Zainal, Development of drug delivery

systems based on layered hydroxides for nanomedicine, Int. J. Mol. Sci. 15 (2014) 7750–7786. https://doi.org/10.3390/ijms15057750.

[13] Y. Zhang, D. Du, X. Li, H. Sun, L. Li, P. Bai, W. Xing, Q. Xue, Z. Yan, Electrostatic Self-Assembly of Sandwich-Like CoAl-LDH/Polypyrrole/Graphene Nanocomposites with Enhanced Capacitive Performance, ACS Appl. Mater. Interfaces. 9 (2017) 31699–31709. https://doi.org/10.1021/acsami.7b04792.

[14] A. Malak-Polaczyk, C. Vix-Guterl, E. Frackowiak, Carbon/layered double hydroxide (LDH) composites for supercapacitor application, Energy and Fuels. 24 (2010) 3346–3351. https://doi.org/10.1021/ef901505c.

[15] P. Vialat, P. Rabu, C. Mousty, F. Leroux, Insight of an easy topochemical oxidative reaction in obtaining high performance electrochemical capacitor based on CoIICoIII monometallic cobalt Layered Double Hydroxide, J. Power Sources. 293 (2015) 1–10. https://doi.org/10.1016/j.jpowsour.2015.05.052.

[16] I. Gualandi, E. Scavetta, Y. Vlamidis, A. Casagrande, D. Tonelli, Co/Al layered double hydroxide coated electrode for in flow amperometric detection of sugars, Electrochim. Acta. 173 (2015) 67–75. https://doi.org/10.1016/j.electacta.2015.04.172.

[17] A. Khenifi, Z. Derriche, C. Forano, V. Prevot, C. Mousty, E. Scavetta, B. Ballarin, L. Guadagnini, D. Tonelli, Glyphosate and glufosinate detection at electrogenerated NiAl-LDH thin films, Anal. Chim. Acta. 654 (2009) 97–102. https://doi.org/10.1016/j.aca.2009.09.023.

[18] H. Farhat, C. Taviot-Gueho, G. Monier, V. Briois, C. Forano, C. Mousty, Insights into the Structure and the Electrochemical Reactivity of Cobalt-Manganese Layered Double Hydroxides: Application to H2O2Sensing, J. Phys. Chem. C. 124 (2020) 15585–15599. https://doi.org/10.1021/acs.jpcc.0c03860.

[19] J. Guo, X. Yang, S. Bai, X. Xiang, R. Luo, J. He, A. Chen, Effect of Mo doping and NiFe-LDH cocatalyst on PEC water oxidation efficiency, J. Colloid Interface Sci. 540 (2019) 9–19. https://doi.org/10.1016/j.jcis.2018.12.069.

[20] Y. Vlamidis, E. Scavetta, M. Gazzano, D. Tonelli, Iron vs Aluminum Based Layered Double Hydroxides as Water Splitting Catalysts, Electrochim. Acta. 188 (2016) 653–660. https://doi.org/10.1016/j.electacta.2015.12.059.

[21] F. Dionigi, Z. Zeng, I. Sinev, T. Merzdorf, S. Deshpande, M.B. Lopez, S. Kunze, I. Zegkinoglou, H. Sarodnik, D. Fan, A. Bergmann, J. Drnec, J.F. de Araujo, M. Gliech, D. Teschner, J. Zhu, W.X. Li, J. Greeley, B.R. Cuenya, P. Strasser, In-situ structure and catalytic

mechanism of NiFe and CoFe layered double hydroxides during oxygen evolution, Nat. Commun. 11 (2020) 1–10. https://doi.org/10.1038/s41467-020-16237-1.

[22] J. Wang, L. Wang, X. Chen, Y. Lu, W. Yang, Chemical power source based on layered double hydroxides, J. Solid State Electrochem. 19 (2015) 1933–1948. https://doi.org/10.1007/s10008-014-2723-5.

[23] D. Du, X. Wu, S. Li, Y. Zhang, W. Xing, L. Li, Q. Xue, P. Bai, Z. Yan, Remarkable supercapacitor performance of petal-like LDHs vertically grown on graphene/polypyrrole nanoflakes, J. Mater. Chem. A. 5 (2017) 8964–8971. https://doi.org/10.1039/c7ta00624a.

[24] E. Scavetta, A. Mignani, D. Prandstraller, D. Tonelli, Electrosynthesis of thin films of Ni, Al hydrotalcite like compounds, Chem. Mater. 19 (2007) 4523–4529. https://doi.org/10.1021/cm071132v.

[25] S. Li, P. Cheng, J. Luo, D. Zhou, W. Xu, J. Li, R. Li, D. Yuan, High-performance flexible asymmetric supercapacitor based on CoAl-LDH and rGO electrodes, Nano-Micro Lett. 9 (2017) 1–10. https://doi.org/10.1007/s40820-017-0134-8.

[26] R. Shan, L. guo Yan, K. Yang, Y. feng Hao, B. Du, Adsorption of Cd(II) by Mg–Al–CO3- and magnetic Fe3O4/Mg–Al–CO3-layered double hydroxides: Kinetic, isothermal, thermodynamic and mechanistic studies, J. Hazard. Mater. 299 (2015) 42–49. https://doi.org/10.1016/j.jhazmat.2015.06.003.

[27] J. He, M. Wei, B. Li, Y. Kang, D.G. Evans, X. Duan, Preparation of layered double hydroxides, Layer. Double Hydroxides. 119 (2006) 89–119. https://doi.org/10.1007/430_006.

[28] D. Tonelli, E. Scavetta, M. Giorgetti, Layered-double-hydroxide-modified electrodes: Electroanalytical applications, Anal. Bioanal. Chem. 405 (2013) 603–614. https://doi.org/10.1007/s00216-012-6586-2.

[29] E. Musella, I. Gualandi, E. Scavetta, A. Rivalta, E. Venuti, M. Christian, V. Morandi, A. Mullaliu, M. Giorgetti, D. Tonelli, Newly developed electrochemical synthesis of Co-based layered double hydroxides: Toward noble metal-free electro-catalysis, J. Mater. Chem. A. 7 (2019) 11241–11249. https://doi.org/10.1039/c8ta11812d.

[30] E. Musella, I. Gualandi, E. Scavetta, M. Gazzano, A. Rivalta, E. Venuti, M. Christian, V. Morandi, D. Tonelli, Electrochemical approach for the production of layered double hydroxides with a well-defined Co/Me(III) ratio, Chem. - A Eur. J. 25 (2019) 16301–16310. https://doi.org/10.1002/chem.201903288.

[31] H. Wang, X. Xiang, F. Li, Facile synthesis and novel electrocatalytic performance of nanostructured Ni-Al layered double hydroxide/carbon nanotube composites, J. Mater. Chem. 20 (2010) 3944–3952. https://doi.org/10.1039/b924911g.

[32] Y. Wang, Z. Chen, H. Li, J. Zhang, X. Yan, K. Jiang, D. den Engelsen, L. Ni, D. Xiang, The synthesis and electrochemical performance of core-shell structured Ni-Al layered double hydroxide/carbon nanotubes composites, Electrochim. Acta. 222 (2016) 185–193. https://doi.org/10.1016/j.electacta.2016.09.073.

[33] I. Gualandi, Y. Vlamidis, L. Mazzei, E. Musella, M. Giorgetti, M. Christian, V. Morandi, E. Scavetta, D. Tonelli, Ni/Al Layered Double Hydroxide and Carbon Nanomaterial Composites for Glucose Sensing, ACS Appl. Nano Mater. 2 (2019) 143–155. https://doi.org/10.1021/acsanm.8b01765.

[34] J.J. Gooding, Nanostructuring electrodes with carbon nanotubes: A review on electrochemistry and applications for sensing, Electrochim. Acta. 50 (2005) 3049–3060. https://doi.org/10.1016/j.electacta.2004.08.052.

[35] M.J. Allen, V.C. Tung, R.B. Kaner, Honeycomb carbon: A review of graphene, Chem. Rev. 110 (2010) 132–145. https://doi.org/10.1021/cr900070d.

[36] D.A.C. Brownson, C.E. Banks, Graphene electrochemistry: an overview of potential applications, Analyst. 135 (2010) 2768. https://doi.org/10.1039/c0an00590h.

[37] M. Pumera, Graphene-based nanomaterials and their electrochemistry, Chem. Soc. Rev. 39 (2010) 4146. https://doi.org/10.1039/c002690p.

[38] L. Zhang, K.N. Hui, K.S. Hui, H. Lee, Facile synthesis of porous CoAl-layered double hydroxide/graphene composite with enhanced capacitive performance for supercapacitors, Electrochim. Acta. 186 (2015) 522–529. https://doi.org/10.1016/j.electacta.2015.11.024.

[39] W. Guo, C. Yu, S. Li, J. Yang, Z. Liu, C. Zhao, H. Huang, M. Zhang, X. Han, Y. Niu, J. Qiu, High-Stacking-Density, Superior-Roughness LDH Bridged with Vertically Aligned Graphene for High-Performance Asymmetric Supercapacitors, Small. 13 (2017) 1–9. https://doi.org/10.1002/smll.201701288.

[40] W. Yang, Z. Gao, J. Wang, J. Ma, M. Zhang, L. Liu, Solvothermal one-step synthesis of Ni-Al layered double hydroxide/carbon nanotube/reduced graphene oxide sheet ternary nanocomposite with ultrahigh capacitance for supercapacitors, ACS Appl. Mater. Interfaces. 5 (2013) 5443–5454. https://doi.org/10.1021/am4003843.

[41] H. Wang, Y. Bai, S. Chen, X. Luo, C. Wu, F. Wu, J. Lu, K. Amine, Binder-free V2O5

cathode for greener rechargeable aluminum battery, ACS Appl. Mater. Interfaces. 7 (2015) 80–84. https://doi.org/10.1021/am508001h.

[42] G.A. Elia, K. Marquardt, K. Hoeppner, S. Fantini, R. Lin, E. Knipping, W. Peters, J.F. Drillet, S. Passerini, R. Hahn, An Overview and Future Perspectives of Aluminum Batteries, Adv. Mater. 28 (2016) 7564–7579. https://doi.org/10.1002/adma.201601357.

[43] R.R. Salunkhe, B.P. Bastakoti, C.T. Hsu, N. Suzuki, J.H. Kim, S.X. Dou, C.C. Hu, Y. Yamauchi, Direct growth of cobalt hydroxide rods on nickel foam and its application for energy storage, Chem. - A Eur. J. 20 (2014) 3084–3088. https://doi.org/10.1002/chem.201303652.

[44] K. Takahashi, Y. Wang, G. Cao, Ni-V 2O 5·nH 2O core-shell nanocable arrays for enhanced electrochemical intercalation, J. Phys. Chem. B. 109 (2005) 48–51. https://doi.org/10.1021/jp044772j.

[45] B. Qu, L. Hu, Q. Li, Y. Wang, L. Chen, T. Wang, High-performance lithium-ion battery anode by direct growth of hierarchical ZnCo2O4 nanostructures on current collectors, ACS Appl. Mater. Interfaces. 6 (2014) 731–736. https://doi.org/10.1021/am405238a.

[46] E. Bernardi, M. Monti, D. Tonelli, P.H. Ho, P. Benito, A. Vaccari, L. Nobili, G. Fornasari, E. Scavetta, Reactions involved in the electrodeposition of hydrotalcite-type compounds on FeCrAlloy foams and plates, Electrochim. Acta. 222 (2016) 1335–1344. https://doi.org/10.1016/j.electacta.2016.11.109.

[47] E. Scavetta, B. Ballarin, M. Giorgetti, I. Carpani, F. Cogo, D. Tonelli, Electrodes modified by One-Step Electrosynthesis of Ni/Al-NO3 Double Layered Hydroxide, J. New Mater. Electrochem. Syst. 7 (2004) 43–50.

[48] N. Muralidharan, R. Essehli, R.P. Hermann, R. Amin, C. Jafta, J. Zhang, J. Liu, Z. Du, H.M. Meyer, E. Self, J. Nanda, I. Belharouak, Lithium Iron Aluminum Nickelate, LiNixFeyAlzO2—New Sustainable Cathodes for Next-Generation Cobalt-Free Li-Ion Batteries, Adv. Mater. 2002960 (2020) 1–13. https://doi.org/10.1002/adma.202002960.

[49] M. Zhao, Q. Zhao, B. Li, H. Xue, H. Pang, C. Chen, Recent progress in layered double hydroxide based materials for electrochemical capacitors: Design, synthesis and performance, Nanoscale. 9 (2017) 15206–15225. https://doi.org/10.1039/c7nr04752e.

[50] E. Scavetta, I. Gualandi, D. Tonelli, C. Mousty, V. Prevot, M. Monti, Electrodeposition of Layered Double Hydroxides on platinum: Insights into the reactions sequence, Electrochim. Acta. 152 (2014) 75–83. https://doi.org/10.1016/j.electacta.2014.11.096.

[51] P.D.T.J. Meyer, H.W.R.J. Sauvage, Layered Double Hydroxides, 2005. https://doi.org/10.1007/b100426.

[52] J. Hu, G. Lei, Z. Lu, K. Liu, S. Sang, H. Liu, Alternating assembly of Ni-Al layered double hydroxide and graphene for high-rate alkaline battery cathode, Chem. Commun. 51 (2015) 9983–9986. https://doi.org/10.1039/c5cc01767j.

[53] J. Pérez-Ramírez, G. Mul, F. Kapteijn, J.A. Moulijn, In situ investigation of the thermal decomposition of Co–Al hydrotalcite in different atmospheres, J. Mater. Chem. 11 (2001) 821–830. https://doi.org/10.1039/b009320n.

[54] C. Ehrhardt, M. Gjikaj, W. Brockner, Thermal decomposition of cobalt nitrato compounds: Preparation of anhydrous cobalt(II)nitrate and its characterisation by Infrared and Raman spectra, Thermochim. Acta. 432 (2005) 36–40. https://doi.org/10.1016/j.tca.2005.04.010.

[55] F. Cavani, F. Trifirò, A. Vaccari, Hydrotalcite-type anionic clays: preparation, properties and applications., Catal. Today. 11 (1991) 173–301. https://doi.org/10.1007/BF03263563.

[56] V.V. Sharma, I. Gualandi, Y. Vlamidis, D. Tonelli, Electrochemical behavior of reduced graphene oxide and multi-walled carbon nanotubes composites for catechol and dopamine oxidation, Electrochim. Acta. 246 (2017) 415–423. https://doi.org/10.1016/j.electacta.2017.06.071.

[57] S.C. Sekhar, G. Nagaraju, J.S. Yu, Conductive silver nanowires-fenced carbon cloth fibers-supported layered double hydroxide nanosheets as a flexible and binder-free electrode for high-performance asymmetric supercapacitors, Nano Energy. 36 (2017) 58–67. https://doi.org/10.1016/j.nanoen.2017.04.019.

[58] A. Shalaby, D. Nihtianova, P. Markov, A.D. Staneva, R.S. Iordanova, Y.B. Dimitriev, Structural analysis of reduced graphene oxide by transmission electron microscopy, Bulg. Chem. Commun. 47 (2015) 291–295.

[59] D.S. Hall, D.J. Lockwood, C. Bock, B.R. MacDougall, Nickel hydroxides and related materials: A review of their structures, synthesis and properties, Proc. R. Soc. A Math. Phys. Eng. Sci. 471 (2015). https://doi.org/10.1098/rspa.2014.0792.

[60] N.S. Mcintyre, M.G. Cook, X-Ray Photoelectron Studies on Some Oxides and Hydroxides of Cobalt, Nickel, and Copper, Anal. Chem. 47 (1975) 2208–2213. https://doi.org/10.1021/ac60363a034.

[61] J.W. Lee, T. Ahn, D. Soundararajan, J.M. Ko, J.D. Kim, Non-aqueous approach to the preparation of reduced graphene oxide/α-Ni(OH)2 hybrid composites and their high capacitance behavior, Chem. Commun. 47 (2011) 6305–6307. https://doi.org/10.1039/c1cc11566a.

[62] J. Liang, M. Renzhi, N. Iyi, Y. Ebina, K. Takada, T. Sasaki, Topochemical synthesis, anion exchange, and exfoliation of Co-Ni layered double hydroxides: A route to positively charged Co-Ni hydroxide nanosheets with tunable composition, Chem. Mater. 22 (2010) 371–378. https://doi.org/10.1021/cm902787u.

[63] H. Jiang, Y. Guo, T. Wang, P.L. Zhu, S. Yu, Y. Yu, X.Z. Fu, R. Sun, C.P. Wong, Electrochemical fabrication of Ni(OH)2/Ni 3D porous composite films as integrated capacitive electrodes, RSC Adv. 5 (2015) 12931–12936. https://doi.org/10.1039/c4ra15092a.

[64] J.T. Kloprogge, L. V. Duong, B.J. Wood, R.L. Frost, XPS study of the major minerals in bauxite: Gibbsite, bayerite and (pseudo-)boehmite, J. Colloid Interface Sci. 296 (2006) 572–576. https://doi.org/10.1016/j.jcis.2005.09.054.

[65] O. Böse, E. Kemnitz, A. Lippitz, W.E.S. Unger, C 1s and Au 4f7/2 referenced XPS binding energy data obtained with different aluminium oxides, -hydroxides and -fluorides, Fresenius. J. Anal. Chem. 358 (1997) 175–179. https://doi.org/10.1007/s002160050376.

[66] L. Zhang, H. Yao, Z. Li, P. Sun, F. Liu, C. Dong, J. Wang, Z. Li, M. Wu, C. Zhang, B. Zhao, Synthesis of delaminated layered double hydroxides and their assembly with graphene oxide for supercapacitor application, J. Alloys Compd. 711 (2017) 31–41. https://doi.org/10.1016/j.jallcom.2017.03.348.

[67] G. Greczynski, L. Hultman, Compromising science by ignorant instrument calibration - need to revisit half a century of published XPS data, Angew. Chemie. (2020). https://doi.org/10.1002/ange.201916000.

[68] N.F. Chiu, C. Du Yang, Real-time and stepwise deoxidization processes to tune the photoluminescence properties of graphene oxide using EC-SPR spectroscopy, RSC Adv. 8 (2018) 11557–11565. https://doi.org/10.1039/c7ra13594g.

[69] https://srdata.nist.gov/xps/main_search_menu.aspx

[70] X. Li, L. Yu, G. Wang, G. Wan, X. Peng, K. Wang, G. Wang, Hierarchical NiAl LDH nanotubes constructed via atomic layer deposition assisted method for high performance supercapacitors, Electrochim. Acta. 255 (2017) 15–22.

https://doi.org/10.1016/j.electacta.2017.09.155.

[71] B. Wang, Q. Liu, Z. Qian, X. Zhang, J. Wang, Z. Li, H. Yan, Z. Gao, F. Zhao, L. Liu, Two steps in situ structure fabrication of Ni-Al layered double hydroxide on Ni foam and its electrochemical performance for supercapacitors, J. Power Sources. 246 (2014) 747–753. https://doi.org/10.1016/j.jpowsour.2013.08.035.

[72] Y. Vlamidis, E. Scavetta, M. Giorgetti, N. Sangiorgi, D. Tonelli, Electrochemically synthesized cobalt redox active layered double hydroxides for supercapacitors development, Appl. Clay Sci. 143 (2017) 151–158. https://doi.org/10.1016/j.clay.2017.03.031.

[73] E. Scavetta, A. Casagrande, I. Gualandi, D. Tonelli, Analytical performances of Ni LDH films electrochemically deposited on Pt surfaces: Phenol and glucose detection, J. Electroanal. Chem. 722–723 (2014) 15–22. https://doi.org/10.1016/j.jelechem.2014.03.018.

[74] B. Wang, Q. Liu, Z. Qian, X. Zhang, J. Wang, Z. Li, H. Yan, Z. Gao, F. Zhao, L. Liu, Two steps in situ structure fabrication of Ni-Al layered double hydroxide on Ni foam and its electrochemical performance for supercapacitors, J. Power Sources. 246 (2014) 747–753. https://doi.org/10.1016/j.jpowsour.2013.08.035.

[75] M. Shao, F. Ning, Y. Zhao, J. Zhao, M. Wei, D.G. Evans, X. Duan, Core-shell layered double hydroxide microspheres with tunable interior architecture for supercapacitors, Chem. Mater. 24 (2012) 1192–1197. https://doi.org/10.1021/cm203831p.

[76] J. Wang, Y. Song, Z. Li, Q. Liu, J. Zhou, X. Jing, M. Zhang, Z. Jiang, In situ Ni/Al layered double hydroxide and its electrochemical capacitance performance, Energy and Fuels. 24 (2010) 6463–6467. https://doi.org/10.1021/ef101150b.

[77] X.M. Liu, Y.H. Zhang, X.G. Zhang, S.Y. Fu, Studies on Me/Al-layered double hydroxides (Me = Ni and Co) as electrode materials for electrochemical capacitors, Electrochim. Acta. 49 (2004) 3137–3141. https://doi.org/10.1016/j.electacta.2004.02.028.

[78] Y. Wei, X. Zhang, X. Wu, D. Tang, K. Cai, Q. Zhang, Carbon quantum dots/Ni-Al layered double hydroxide composite for high-performance supercapacitors, RSC Adv. 6 (2016) 39317–39322. https://doi.org/10.1039/c6ra02730j.

[79] L. Zhang, J. Wang, J. Zhu, X. Zhang, K. San Hui, K.N. Hui, 3D porous layered double hydroxides grown on graphene as advanced electrochemical pseudocapacitor materials, J. Mater. Chem. A. 1 (2013) 9046–9053. https://doi.org/10.1039/c3ta11755c.

[80] L. Zhang, M. Ou, H. Yao, Z. Li, D. Qu, F. Liu, J. Wang, J. Wang, Z. Li, Enhanced

supercapacitive performance of graphite-like C3N4 assembled with NiAl-layered double hydroxide, Electrochim. Acta. 186 (2015) 292–301. https://doi.org/10.1016/j.electacta.2015.10.192.

[81] L. Zhang, K.N. Hui, K.S. Hui, X. Chen, R. Chen, H. Lee, Role of graphene on hierarchical flower-like NiAl layered double hydroxide-nickel foam-graphene as binder-free electrode for high-rate hybrid supercapacitor, Int. J. Hydrogen Energy. 41 (2016) 9443–9453. https://doi.org/10.1016/j.ijhydene.2016.04.050.

[82] X. Ge, C. Gu, Z. Yin, X. Wang, J. Tu, J. Li, Periodic stacking of 2D charged sheets: Self-assembled superlattice of Ni-Al layered double hydroxide (LDH) and reduced graphene oxide, Nano Energy. 20 (2016) 185–193. https://doi.org/10.1016/j.nanoen.2015.12.020.